



ANALYTICAL MODEL FOR UNCONFINED AND CONFINED HIGH STRENGTH CONCRETE UNDER CYCLIC LOADING

Dimitrios KONSTANTINIDIS¹, Andreas J. KAPPOS² and Bassam A. IZZUDDIN³

SUMMARY

A previously proposed model for uniaxial loading of confined high strength concrete (HSC) is extended in this paper to include cyclic loading. Parameters such as, compressive strength, volumetric ratio of transverse reinforcement, yield strength of ties, tie spacing, and tie pattern, dissipation of energy through the hysteresis loops, stiffness degradation as damage progresses, degree of confinement, and ductility are all taken into account. Comparison of the results from finite element analysis using ADAPTIC, in which the proposed material model is implemented, against experimental results demonstrated good agreement, thus paving the way for much needed parametric studies on the behavior of structures made of HSC.

INTRODUCTION

Reinforced Concrete (RC) has been widely used as a construction material in earthquake prone areas because of its low cost, excellent durability and ease of maintenance. In recent years development of mineral and chemical admixtures have made it possible to produce high strength concrete (HSC), while steel manufacturers have developed high yield steel (HYS) to be used as longitudinal and transverse reinforcement for RC structures in seismic zones. These developments were the results of forecasts that high strength materials (HSM) will provide exceptional benefits for high-rise buildings, long-span bridges, tunnels, tanks and off shore platforms.

In the design of earthquake resistant of RC structures, ductility is a fundamental requirement, which is determined either as the ability of structural members to undergo large inelastic deformations without significant loss in strength, or as the ability of members to dissipate the imposed seismic energy. It is the confinement that influences the behavior of structural elements, particularly in plastic hinge regions, consequently affecting the overall behavior of the structural system to a considerable extent. The ability of the members to withstand forces after spalling of the concrete cover relies on the confinement stresses induced in the core. The effectiveness of confinement depends on the compressive strength of concrete, the amount of transverse reinforcement, the yield strength of transverse reinforcement, the spacing of the ties, the tie pattern, the longitudinal reinforcement, the rate of loading and the strain gradient. Therefore, an accurate mathematical model of the stress-strain response of RC members under load reversals should

¹ Structural Engineer, Egnatia Odos A.E., Thessaloniki, Greece. Email: dkon@egnatia.gr

² Professor, Aristotle University of Thessaloniki, Dept. of Civil Engrg, Greece. Email: ajkap@civil.auth.gr

³ Reader, Imperial College, Dept. of Civil and Envrml Engrg, London, UK. Email: b.izzuddin@imperial.ac.uk

account for all these parameters. Such a model for confined and unconfined HSC under cyclic loading is presented and validated in this paper.

REVIEW OF ANALYTICAL MODELS FOR CYCLIC LOADING

For the development of an analytical model for concrete under cyclic loading, it has been shown that it is more important to accurately describe the envelope curve rather than the shape of the unloading and reloading branches (Penelis and Kappos [1]). This is verified by Figure 1, which illustrates the stress-strain diagram of a square specimen with 57 MPa concrete strength subjected to repeated uniaxial compression as reported by Muguruma et al. [2], as well as the stress-strain curve of the same specimen tested under monotonically increasing compressive loading. It can be seen from the figure that the stress-strain curve of HSC under cyclic loading practically coincides with the curve resulting from monotonic application of the loading. Similar results for normal strength concrete were reported by Karsan and Jirsa [3]. Other parameters that ought to be accounted for include the degradation of stiffness and strength, the increase in concrete plastic strain ϵ_{pl} , as well as the effect of confinement provided by transverse reinforcement.

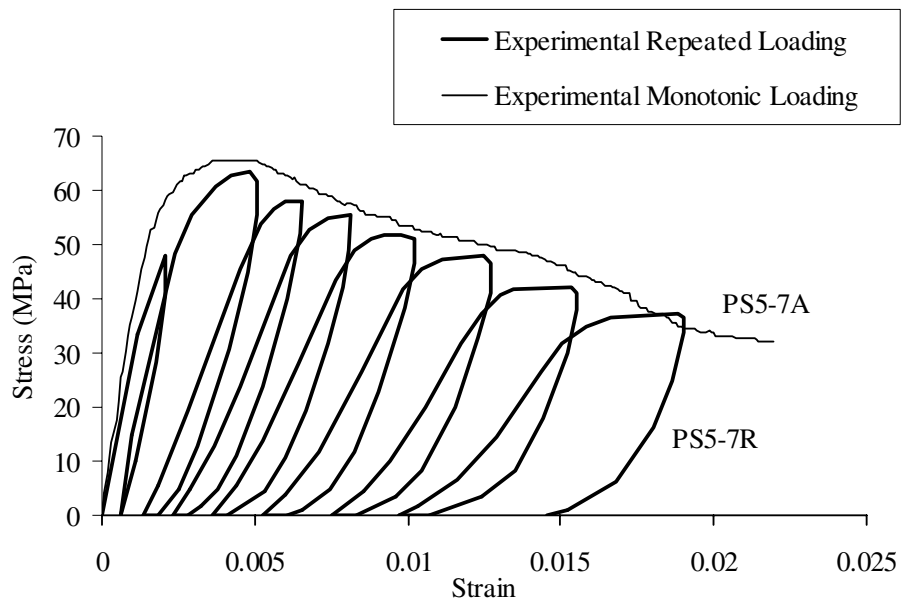
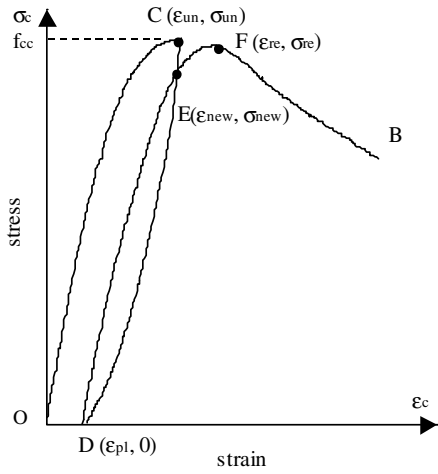


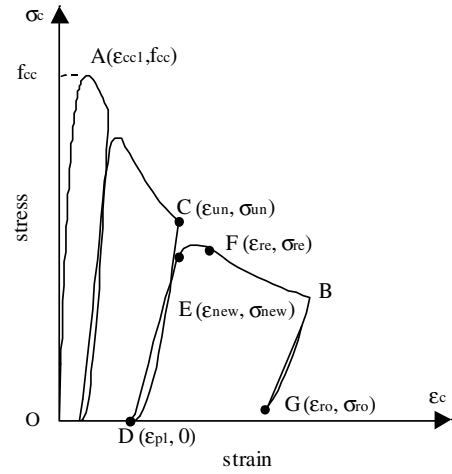
Figure 1. Stress-strain diagram for HSC specimen subjected to repeated uniaxial compression

Aoyama and Noguchi [4], summarized a number of models that have been developed to predict the response of concrete under cyclic loading. Neither these analytical models nor the more recent ones by Yankelevsky and Reinhardt [5], Mander et al. [6], Otter and Naaman [7], Martinez-Rueda [8] have been developed for HSC.

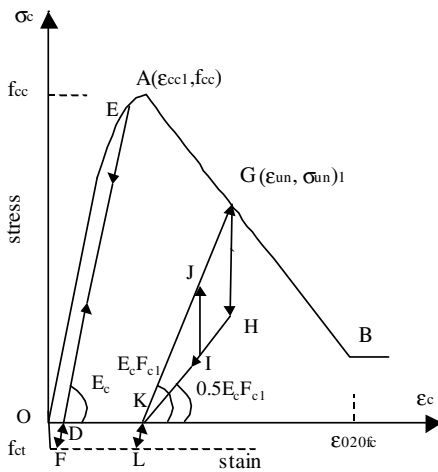
In Figure 2, the stress-strain diagrams of five well-known models for the cyclic behavior of normal strength concrete are illustrated, while Table 1 presents the main parameters of six models developed for NSC. As can be seen from Table 1, the Yankelevsky and Reinhardt [5], as well as the Otter and Naaman [7] models can be tailored to any stress-strain curve for the description of the monotonic behavior of concrete, as they are independent of the envelope curve.



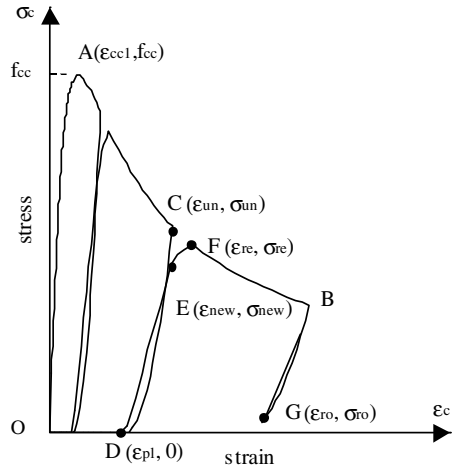
a) Karsan and Jirsa model [3]



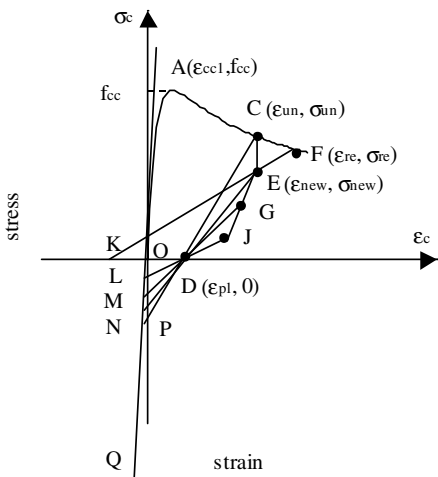
d) Mander et al. model [6]



b) Blakeley and Park model [9]



e) Martinez - Rueda model [8]



c) Yankelevsky and Reinhardt model [5]

Figure 2. Analytical stress-strain curves for cyclic behaviour of concrete

Following tests on short rectangular columns, Karsan and Jirsa [3] observed that in the stress-strain diagram there is a locus of common points which is defined by the intersection of the loading and reloading branches (ϵ_{new} , σ_{new}). All models considered herein, except those of Blakeley and Park [9] and Otter and Naaman [7] acknowledge this observation. In the model shown in Figure 2a, which did not take into account the confinement effect, the relationship for the unloading branch is a second degree parabola passing through the point where unloading commences (ϵ_{un} , σ_{un}), also called the strain reversal point, the common point (ϵ_{new} , σ_{new}), and the full reversal point (ϵ_{pl} , 0). The expression for reloading is a second degree parabola passing through the full reversal point (ϵ_{pl} , 0), the common point (ϵ_{new} , σ_{new}), and the returning point (ϵ_{re} , σ_{re}).

Blakeley and Park [9] developed a more simplified concrete model shown in Figure 2b, which provided equations for an envelope that also ignored the effect of confinement. This model assumes that unloading and reloading take place along a line without energy dissipation or stiffness deterioration for strains smaller or equal to the strain corresponding to peak stress ($\epsilon_c \leq \epsilon_{c1}$). Beyond this point, stiffness degradation is considered by the introduction of the reduction function F_c given in Table 1. Along the first branch of unloading, stress is reduced to 50 percent without any reduction in strain (point H on line GH). The second branch is a straight line with slope equal to $0.50F_c E_c$ passing through points H mentioned above and K, which is the intersection point with the strain axis (i.e. zero stress). If cracking has not occurred tensile stresses can develop (line KL), otherwise strain decreases with zero stress. Reloading is assumed to take place along the straight line KG with slope equal to $F_c E_c$ until the envelope is reached. If reloading starts prior to reaching zero stress, then the first line to be followed is parallel to the initial unloading branch (line IJ).

The phenomenological model proposed by Yankelevsky and Reinhardt [5], shown in Figure 2c, focuses on describing the unloading and reloading branches, which are presented as piece-wise linear, while the envelope is assumed to be given. The concept of the model is based on the observation that unloading from the envelope curve exhibits rather high stiffness at low strain reversals, which then softens sharply with further unloading. As the model laws are formulated using the equations given in Table 1 for plastic strain, the common and reloading point can vary for different envelope curves. The equations presented in Table 1 are set up assuming linear relationships for the envelope.

The model presented by Mander et al. [6] shown in Figure 2d is a simplified version of the Karsan and Jirsa [3] model that also models the capability of concrete to carry some tensile stresses. The envelope curve is assumed to be given by the Popovic equation [10], which also accounts for the effect of confinement. The unloading curves adopted are second degrees parabolas joining the strain reversal point (ϵ_{un} , σ_{un}) with the current full reversal point (ϵ_{pl} , 0) with zero slope. Reloading takes place along two branches. For strains smaller than the maximum strain experienced (ϵ_{un}) a straight line was fitted between the reloading point (ϵ_{ro} , σ_{ro}) and the degrading strength point (ϵ_{new} , σ_{new}). For strains larger than ϵ_{un} , a parabolic curve connects the descending strength point (ϵ_{new} , σ_{new}) and the returning point (ϵ_{re} , σ_{re}) lying on the envelope. The equation for the inelastic strain ϵ_{pl} is given in Table 1 and is updated every time the maximum strain experienced ϵ_{un} is altered. Therefore this updating procedure may take place either along the envelope or along the second reloading branch.

Martinez-Rueda [8] modified Mander's et al. [6] model based on the observed lack of numerical stability of Mander's model particularly under large displacements, which caused convergence problems when implemented into a non-linear program following a fiber element approach. Among the modifications made was the introduction of three different definitions of plastic strain ϵ_{pl} corresponding to low, intermediate and high strain range and accounting for the softening of concrete with progression of strains (Figure 2e).

Table 1. Summary of models for cyclic behavior of concrete

Model	Envelope Curve	Plastic strain, Common & Reloading Point	Unloading & Reloading curves
Karsan and Jirsa [3]	$\sigma = 0.85f_c \frac{\epsilon}{\epsilon_{cc1}} e^{\left(1 - \frac{\epsilon}{\epsilon_{cc1}}\right)}$	$\epsilon_{pl} = \epsilon_{cc1} (1.76 - \beta) \left[0.16 \left(\frac{\epsilon_{new}}{\epsilon_{cc1}} \right)^2 + 0.133 \left(\frac{\epsilon_{new}}{\epsilon_{cc1}} \right) \right]$ $\sigma_{new} = f_{cc} \beta \frac{\epsilon_{new}}{\epsilon_{cc1} (0.315 + 0.77\beta)} e^{\left(1 - \frac{\epsilon_{new}}{\epsilon_{cc1} (0.315 + 0.77\beta)}\right)}$ $\beta = 0.76$	<u>Unloading branch</u> $\sigma = f_c \left[0.093 \left(\frac{\epsilon_{un}}{\epsilon_{cc1}} \right)^2 + 0.091 \left(\frac{\epsilon_{un}}{\epsilon_{cc1}} \right) \right]$ <u>Reloading branch</u> $\sigma = f_c \left[0.145 \left(\frac{\epsilon_{un}}{\epsilon_{cc1}} \right)^2 + 0.13 \left(\frac{\epsilon_{un}}{\epsilon_{cc1}} \right) \right]$
Blakeley and Park [9]	<ul style="list-style-type: none"> for $0 \leq \epsilon \leq \epsilon_{cc1}$ $\sigma = f_c \left[\frac{2\epsilon}{\epsilon_{c1}} - \left(\frac{\epsilon}{\epsilon_{c1}} \right)^2 \right]$ for $\epsilon \geq \epsilon_{cc1}$ $\sigma = f_c \left[1 - \frac{0.5}{\epsilon_{0.50fc} - \epsilon_{c1}} (\epsilon - \epsilon_{c1}) \right]$ 	ϵ_{pl} is defined graphically $\epsilon_{re} = \epsilon_{un}$ $F_c = 0.80 - \frac{0.7(\epsilon_{un} - \epsilon_{c1})}{\epsilon_{0.20fc} - \epsilon_{c1}} \geq 0.1$	<u>Unloading branch</u> <ul style="list-style-type: none"> for $0 \leq \epsilon \leq \epsilon_{cc1}$ straight line with slope E_c for $\epsilon \geq \epsilon_{cc1}$ 1^{st} branch: straight line vertical to the strain axis 2^{nd} branch: straight line with slope $0.50E_c F_c$ <u>Reloading branch</u> <ul style="list-style-type: none"> for $0 \leq \epsilon \leq \epsilon_{cc1}$ - straight line with slope E_c for $\epsilon \geq \epsilon_{cc1}$ - straight line with slope $E_c F_c$
Yankelevsky and Reinhardt [5]	Any curve for the uniaxial response of concrete	$\epsilon_{pl} = \epsilon_{un} - \frac{\sigma_{un} \left(\frac{f_{cc}}{E_c} + \epsilon_{un} \right)}{f_{cc} + \sigma_{un}}$ $\sigma_{new} = \frac{0.75f_{cc} (\epsilon_{un} - \epsilon_{pl})}{\frac{0.75f_{cc}}{E_c} + \epsilon_{pl}} \quad \epsilon_{new} = \epsilon_{un}$ $\sigma_{re} = \sigma_{new} + \sigma_{new} \left(\frac{\epsilon_{re} - \epsilon_{un}}{\epsilon_{cc1} + \epsilon_{un}} \right), \epsilon_{re} \text{ defined from the envelope}$	<u>Unloading branch</u> 1^{st} branch - straight line vertical to the strain axis (CE) 2^{nd} branch - straight line (EJ) 3^{rd} branch - straight line (JD) <u>Reloading branch</u> 1^{st} branch - straight line (DE) 2^{nd} branch - straight line (EF)
Mander et. al. [6]	$\sigma = \frac{f_{cc} \frac{\epsilon}{\epsilon_{cc1}} r}{r - 1 + \left(\frac{\epsilon}{\epsilon_{cc1}} \right)^r}$ $r = \frac{E_c}{E_c - E_{c1}}$	$\epsilon_{pl} = \epsilon_{un} - \frac{\epsilon_{un} + \epsilon_a}{\sigma_{un} + E_c \epsilon_a} \quad \epsilon_a = a \sqrt{\epsilon_{un} \epsilon_{cc1}}$ $a = \max \left\{ \frac{\epsilon_{cc1}}{\epsilon_{cc1} + \epsilon_{un}}; \frac{0.9\epsilon_{un}}{\epsilon_{cc1}} \right\}$ $\sigma_{new} = 0.92\sigma_{un} + 0.08\sigma_{ro} \quad \epsilon_{new} = \epsilon_{un}$ $\epsilon_{re} = \epsilon_{un} + \frac{\sigma_{un} - \sigma_{new}}{E_r \left(2 + \frac{f_{cc}}{f_c} \right)} \quad E_r = \frac{\sigma_{ro} - \sigma_{new}}{\epsilon_{ro} - \epsilon_{un}} \quad E_{re} = \frac{\sigma_{re} - \sigma_{new}}{\epsilon_{re} - \epsilon_{un}}$	<u>Unloading branch</u> $\sigma = \sigma_{un} - \frac{\sigma_{un} \left(\frac{\epsilon - \epsilon_{un}}{\epsilon_{pl} - \epsilon_{un}} \right) \frac{bcE_c}{bcE_c - E_{c1}}}{\frac{bcE_c}{bcE_c - E_{c1}} - 1 + \left(\frac{\epsilon - \epsilon_{un}}{\epsilon_{pl} - \epsilon_{un}} \right)^{\frac{bcE_c}{bcE_c - E_{c1}}}}$ <u>Reloading branch</u> 1^{st} branch $\sigma = \sigma_{ro} + E_r (\epsilon - \epsilon_{ro})$ 2^{nd} branch $\sigma = \sigma_{re} + E_r (\epsilon - \epsilon_{re}) + A (\epsilon - \epsilon_{re})^2$ $b = \frac{\sigma_{un}}{f_c} \geq 1 \quad c = \sqrt{\frac{\epsilon_{cc1}}{\epsilon_{un}}} \leq 1 \quad E_{c1} = \frac{\sigma_{un}}{\epsilon_{un} - \epsilon_{pl}}$
Otter and Naaman [7]	Any curve for the uniaxial response of concrete	$\epsilon_{pl} = \epsilon_{c1} \left[\frac{\epsilon_{un}}{\epsilon_{cc1}} - k_u \left(1 - e^{-\frac{\epsilon_{un}}{k_u \epsilon_{cc1}}} \right) \right] \quad k_u = 0.80$ $\epsilon_{re} = \epsilon_{cc1} \left(\frac{\epsilon_{un}}{\epsilon_{cc1}} + k_r \right)$ $k_r = 0.1$ for plain and fibre-reinforced concrete	<u>Unloading branch</u> $\sigma = \sigma_{un} \left(1 - p \right) \left(\frac{\epsilon - \epsilon_{pl}}{\epsilon_{un} - \epsilon_{pl}} \right) + p \left(\frac{\epsilon - \epsilon_{pl}}{\epsilon_{un} - \epsilon_{pl}} \right)^{n_u}$ $p = 0.9; n_u = 3$ derived fitting exp. data <u>Reloading branch</u> $\sigma = \sigma_{un} \left(\frac{\epsilon - \epsilon_{pl}}{\epsilon_{re} - \epsilon_{pl}} \right)$
Martinez - Rueda [8]	$\sigma = \frac{f_{cc} \frac{\epsilon}{\epsilon_{cc1}} r}{r - 1 + \left(\frac{\epsilon}{\epsilon_{cc1}} \right)^r}$ $r = \frac{E_c}{E_c - E_{c1}}$	<ul style="list-style-type: none"> for $0 \leq \epsilon_{un} \leq \epsilon_{0.35fc}$ $\epsilon_{pl} = \epsilon_{un} - \frac{\sigma_{un}}{E_c}$ for $\epsilon_{0.35fc} < \epsilon_{un} \leq 2.5\epsilon_{cc1}$ $\epsilon_{pl} = \epsilon_{un} - \frac{\epsilon_{un} + \epsilon_a}{\sigma_{un} + E_c \epsilon_a}$ for $2.5\epsilon_{cc1} \leq \epsilon_{un}$ $\epsilon_{pl} = \frac{\sigma_{cr} \epsilon_{un} - \sigma_{un} \epsilon_f }{\sigma_{cr} + \sigma_{un}}$ $\sigma_{new} = \frac{0.9f_{cc} \frac{\epsilon_c}{0.9 \epsilon_{cc1}} r}{r - 1 + \left(\frac{\epsilon_c}{\epsilon_{cc1}} \right)^r} \quad \epsilon_{new} = \epsilon_{un}$ $\epsilon_{re} = \frac{\epsilon'_{re} + \epsilon_{un}}{2} \quad \epsilon'_{re} = \left(0.00273 + 1.2651 \frac{\epsilon_{un}}{\epsilon_{cc1}} \right) \epsilon_{un}$	<u>Unloading branch</u> $\sigma = \sigma_{un} \left(\frac{\epsilon - \epsilon_{pl}}{\epsilon_{un} - \epsilon_{pl}} \right)^2$ <u>Reloading branch</u> 1^{st} branch $\sigma = \sigma_{ro} + E_r (\epsilon - \epsilon_{ro})$ 2^{nd} branch $\sigma = \sigma_{new} + E_{re} (\epsilon - \epsilon_{re})$ $\sigma_{cr} = \frac{2.5f_{cc} r}{r - 1 + 2.5^r} \quad \epsilon_{cr} = 2.5 \epsilon_{cc1}$

The second reloading branch (i.e. for strains larger than ε_{un}) was also transformed to a straight line between the reduced strength point (ε_{new} , σ_{new}) and the returning point (ε_{re} , σ_{re}). To compensate for the lack of a smooth transition between the reloading branches and the envelope, the returning strain ε_{re} was set to the average value between ε_{new} and the returning strain ε'_{re} (see Table 1), which is obtained using the empirical equations of Karsan and Jirsa [3].

The Otter and Naaman [7] model was originally developed for plain and fiber-reinforced concrete, but can also be applied to confined concrete with little modification. The model uses the unloading strain, the plastic strain and the reloading point as end-points of the unloading and reloading curves. The unloading curve is described by a polynomial equation, where functions p and n_{uc} (see Table 1) were derived by fitting experimental results. A simpler equation is proposed for the reloading branch consisting of one linear expression. Finally, in the equation for plastic strain ε_{pl} the parameters k_u and k_r (see Table 1) were derived for fiber-reinforced concrete, while no suggestion was made for reinforced concrete.

MODEL FOR UNCONFINED AND CONFINED HSC UNDER CYCLIC LOADING

The proposed model for unconfined and confined HSC under cyclic loading is essentially an extension of the analytical model proposed by Kappos and Konstantinidis [11] for uniaxial loading, which incorporates essential phenomenological parameters and enhances the accuracy in predicting the monotonic stress-strain behavior of HSC, having been tailored to a modified version of the cyclic rules proposed by Mander et al. [6] as revised by Martinez-Rueda [8]. This advanced analytical model takes into account dissipation of energy through the hysteresis loops, stiffness degradation as damage progresses, the confinement effect on strength as well as ductility, and is used in parametric analyses of the performance of HSC members, subassemblies and assessment of structures under simulated seismic loads.

Envelope Curve

Previous experimental investigations by Karsan and Jirsa [3] concluded that the stress-strain envelope curve of NSC under repeated or cyclic compressive loading nearly coincides with the stress-strain response under uniaxial loading. A similar observation has also been made for HSC columns confined with HYS by Bing et al. [12].

In line with these observations, the three-branch stress-strain curve (equations 1 and 2) proposed by Kappos and Konstantinidis [11] to model the response of HSC under uniaxial loading, forms the envelope curve to the cyclic loading stress-strain response, both for confined and unconfined HSC.

Ascending branch

$$0 < \varepsilon_c \leq \varepsilon_{cc1} \quad \sigma_c = \frac{f_{cc} \frac{\varepsilon_c}{\varepsilon_{cc1}} \frac{E_c}{E_c - E_{c1}}}{\frac{E_c}{E_c - E_{c1}} - 1 + \left(\frac{\varepsilon_c}{\varepsilon_{cc1}} \right)^{\frac{E_c}{E_c - E_{c1}}}} \quad (1)$$

Descending branch

$$\varepsilon_c > \varepsilon_{cc1} \quad \sigma_c = f_{cc} \left[1 - 0.5 \frac{\varepsilon_c - \varepsilon_{cc1}}{\varepsilon_{0.50f_{cc}} - \varepsilon_{cc1}} \right] \geq 0.3f_{cc} \quad (2)$$

The modulus of elasticity of concrete is assumed to be given by the relationship suggested by the CEB Working Group on HSC/HPC [13].

$$E_c = 22000 \left(\frac{f_c}{10} \right)^{0.3} \quad (\text{MPa}) \quad (3)$$

while the secant modulus of elasticity at peak stress is

$$E_{c1} = \frac{f_{cc}}{\varepsilon_{cc1}} \quad (\text{MPa}) \quad (4)$$

In the case of confined HSC members the peak stress is given by equation 5, which assumes that the compressive strength in a member of usual slenderness is 15 percent lower than the corresponding strength of a shorter test cylinder. This assumption is a result of the difference in size and shape, less effective compaction, water segregation etc., which occur in a full size member (Martinez, Nilson and Slate [14], Cusson and Paultre [15]). The maximum strength for unconfined HSC is assumed to be that corresponding to the strength specified in standard cylinders, i.e. 150 x 300 mm.

$$f_{cc} = 0.85f_c + 10.3 (\alpha \rho_w f_{yw})^{0.4} \quad (\text{MPa}) \quad (5)$$

α is the modified Sheikh and Uzumeri [16] factor for calculating the effectiveness of confinement given by the following formula.

$$\alpha = \left(1 - \frac{\sum b_i^2}{6b_c d_c} \right) \left(1 - \frac{s}{2b_c} \right) \left(1 - \frac{s}{2d_c} \right) \quad (6)$$

where b_i is the center-to-center distance between laterally supported longitudinal bars, b_c and d_c the center-to-center width and height of the perimeter tie respectively and s the spacing between the ties.

The strain at peak stress of confined HSC (ε_{cc1}) is assumed to be given by equation 7,

$$\frac{\varepsilon_{cc1}}{\varepsilon_{c1}} = 1 + 32.8 (\alpha \omega_w)^{1.9} \quad (7)$$

where the mechanical ratio of transverse reinforcement is given by

$$\omega_w = \frac{\rho_w f_{yw}}{f_c} \quad (8)$$

while the strain at peak stress for the unconfined HSC (ε_{c1}) is that given by equation 9.

$$\varepsilon_{c1} = \frac{0.70f_c^{0.31}}{1000} \quad (9)$$

The strain corresponding to a drop in maximum stress by fifty percent, which determines the slope of the descending branch, is given by equation 10 for confined HSC,

$$\varepsilon_{0.50fcc} = \varepsilon_{c1} + 0.091 (\alpha \omega_w)^{0.8} \quad (10)$$

while for the unconfined concrete equation 11 proposed in the CEB Model Code 1990 [17] is adopted.

$$\varepsilon_{0.50fc} = \left[\frac{E_c}{2E_{c1}} + 1 + \sqrt{\left(\frac{E_c}{2E_{c1}} + 1 \right)^2 - 2} \right] \frac{\varepsilon_{c1}}{2} \quad (11)$$

Figure 3 illustrates the envelope curves for confined and unconfined HSC.

Plastic Strain

The 'plastic' strain ε_{pl} , better referred to (in the case of concrete) as the non-recoverable strain, is the strain corresponding to zero stress on the compressive unloading or reloading curves reflecting the accumulation

of damage in a member and defining the strength and stiffness degradation due to cyclic loading. Mander et al. [6] used the same relationship for plastic strain throughout the cyclic history (see also Table 1), while Martinez-Rueda [8] proposed three different equations reflecting the level of damage of the member corresponding to low, intermediate and high strain range and depending on the reversal point from the envelope (ϵ_{un} , σ_{un}). It is pointed out that the value of plastic strain (ϵ_{pl}) is recalculated whenever the reversal point is updated.

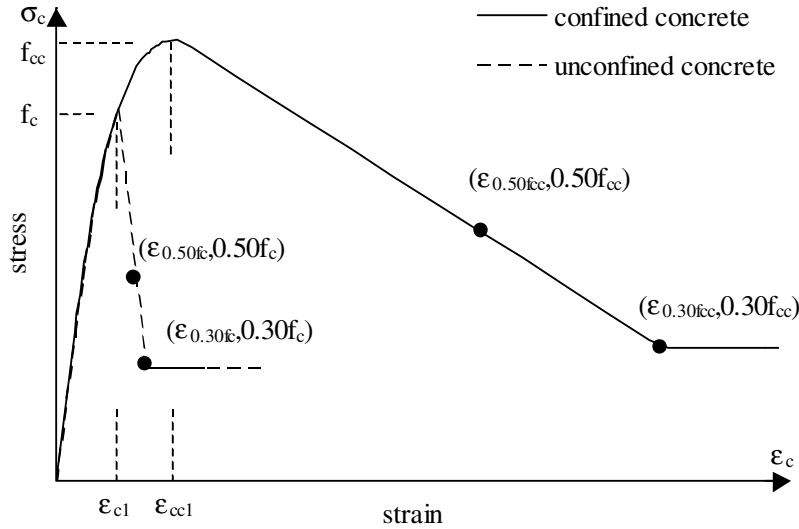


Figure 3. Envelope curves for unconfined and confined HSC

(a) Low Strain Range

The response of concrete is essentially elastic when unloading occurs within the range of strains from the origin up to the strain corresponding to a stress equal to 35% of maximum strength ($\epsilon_{0.35f_{cc}}$) along the ascending branch (Figure 4). Therefore, plastic strains can be obtained from:

$$0 \leq \epsilon_{un} \leq \epsilon_{0.35f_{cc}} \quad \epsilon_{pl} = \epsilon_{un} - \frac{\sigma_{un}}{E_c} \quad (12)$$

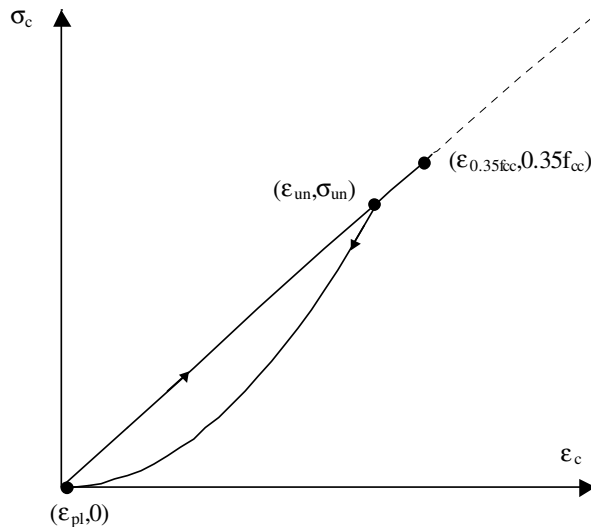


Figure 4. Plastic strain in the low strain range

(b) *Intermediate and High Strain Range*

Figure 5 shows the proposal of Mander et al. [6] for the determination of plastic strain, which was adopted by Martinez-Rueda [8] for the intermediate strain range i.e. for $\epsilon_{0.35f_{cc}} < \epsilon_{un} \leq 2.5\epsilon_{cc1}$. It is seen from the figure that point $(\epsilon_{pl}, 0)$ lies on the line determined by the reversal point from the envelope $(\epsilon_{un}, \sigma_{un})$ and the focal point (ϵ_a, σ_f) , which in turn lies on the line passing through the origin with slope equal to the tangent modulus (E_c) . By combining the equations for the two lines, plastic strain can be specified as follows:

$$\epsilon_{0.35f_{cc}} < \epsilon_{un} \quad \epsilon_{pl} = \epsilon_{un} - \frac{\sigma_{un}(\epsilon_{un} + \epsilon_a)}{\sigma_{un} + E_c \epsilon_a} \quad (13)$$

where ϵ_a is given by the following equation,

$$\epsilon_a = a\sqrt{\epsilon_{un}\epsilon_{cc1}} \quad (14)$$

and a is the maximum value of the two ratios written below, proposed by Mander et al. [6], which, in the absence of more refined values, are also adopted for HSC:

$$a = \max \left\{ \begin{array}{l} \frac{\epsilon_{cc1}}{\epsilon_{cc1} + \epsilon_{un}} \\ \frac{0.09\epsilon_{un}}{\epsilon_{cc1}} \end{array} \right. \quad (15)$$

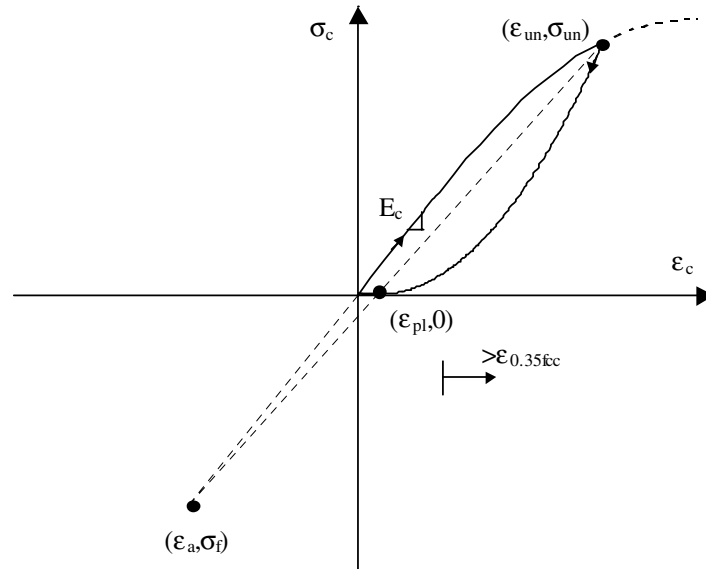


Figure 5. Plastic strain in the intermediate and high strain range

The third equation for plastic strain (ϵ_{pl}) proposed by Martinez-Rueda [8] for unloading from the envelope when strains are greater than 2.5 times ϵ_{cc1} was also examined. However, it is not included in the present model due to the analytical problems resulting from the use of two different equations to describe the descending branch of the envelope curve instead of using only one as was the case in the Martinez-Rueda proposal.

Unloading Branches

The equation describing the unloading branch is a second-degree parabola passing through the reversal point from the envelope $(\epsilon_{un}, \sigma_{un})$ and the current plastic strain point $(\epsilon_{pl}, 0)$, as shown in Figure 4:

$$\sigma_c = \sigma_{un} \left(\frac{\epsilon_c - \epsilon_{pl}}{\epsilon_{un} - \epsilon_{pl}} \right)^2 \quad (16)$$

Reloading Branches

Reloading is assumed to occur along a straight line passing through the reloading point from the unloading curve $(\epsilon_{ro}, \sigma_{ro})$ and the returning point $(\epsilon_{re}, \sigma_{re})$, which coincides with the unloading from the envelope point $(\epsilon_{un}, \sigma_{un})$. The reader is reminded that Martinez-Rueda [8] used two straight lines to describe the reloading branch (see also Figure 2). For strains smaller than the strain ϵ_{un} at which unloading from the envelope commences, a straight line was fitted between the reloading point $(\epsilon_{ro}, \sigma_{ro})$ and the degrading strength point $(\epsilon_{new}, \sigma_{new})$. For strains larger than ϵ_{un} , a straight line was fitted between the reduced strength point $(\epsilon_{new}, \sigma_{new})$ and the returning point $(\epsilon_{re}, \sigma_{re})$. The inconvenience of such a formulation (i.e. significant increase in computation time when modeling involves a large number of elements) and the fact that empirical data used by Martinez-Rueda were not verified for HSC, led to the simplification of the reloading branch in the proposed model, as illustrated in Figure 6.

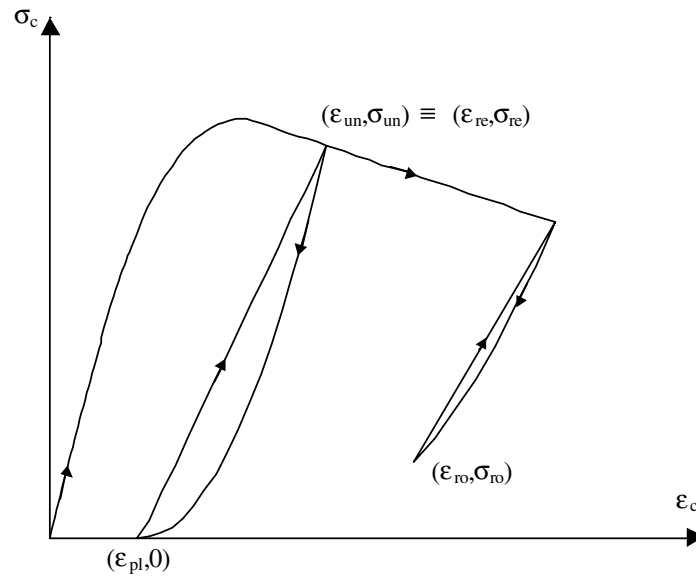


Figure 6. Reloading branches

Tensile Unloading Branches

The relationship for tensile concrete stress (σ_{ct}) , when unloading from a compressive branch is given by equation 17.

$$\sigma_{ct} = f'_{ct} \left(1 - \frac{\epsilon_{pl}}{\epsilon_{cc1}} \right) \quad (17)$$

where f'_{ct} is the tensile concrete strength.

If $\epsilon_{pl} > \epsilon_{cc1}$ then $\sigma_{ct} = 0$

If $\epsilon_{pl} < \epsilon_{cc1}$ the stress-strain relation becomes:

$$\sigma_c = E_t (\epsilon_c - \epsilon_{pl}) \quad (18)$$

where

$$E_t = \frac{\sigma_{ct}}{\varepsilon_t} \quad (19)$$

$$\varepsilon_t = \frac{f'_{ct}}{E_c} \quad (20)$$

When the tensile strain at tensile strength is exceeded, i.e. $\varepsilon_c > (\varepsilon_t - \varepsilon_{pl})$, cracks open and the tensile strength of concrete for the subsequent loading is assumed to be zero (Figure 7).

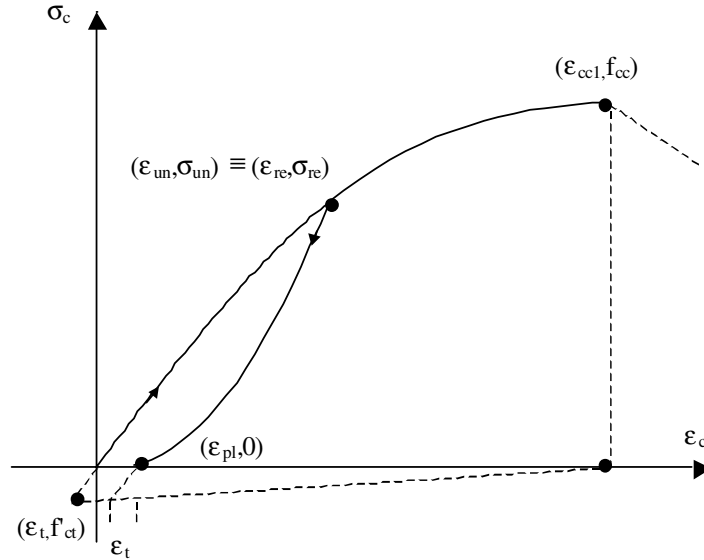


Figure 7. Deterioration in tensile concrete strength due to prior compression loading

VALIDATION UNDER CYCLIC LOADING

Specimen D60-15-4-2 5/8-0.2P reported by Azizinamini et al. [18] is used to validate the proposed model, as implemented for the cubic fiber-type element within ADAPTIC (Izzuddin [19]). The specimen had a cross-section of 305 x 305 mm and a height of 2440 mm, representing a two-third scaled model of a prototype column. The compressive strength of concrete specified in 100 x 200 mm cylinders was reported to be 100.8 MPa, yielding a converted standard cylinder strength of 95.7 MPa (Cook [20]). Ties with yield strength of 453 MPa provided confinement to the core of the column, while longitudinal reinforcement consisted of eight bars of 473 MPa yield strength. Prior to application of the horizontal load reversals, the specimen was subjected first to an axial load (reported value of $0.2 f_c A_g$).

In terms of finite element modeling, the column is represented with nineteen cubic elasto-plastic elements over one half of the specimen. Since the two columns, above and below the stub, had slightly different lengths, the modeled length of the column was the mean value. The value of the tensile concrete strength (f'_{ct}) is assumed to be 5.1 MPa, which is the suggested value of the CEB Working Group on HSC/HPC [13]. The remaining parameters for concrete are estimated using the proposed equations, while the longitudinal steel reinforcement is modeled using a bilinear model. Figure 8 shows the comparison between the analytical and the experimental results. It is notable that the proposed model for HSC is capable of predicting the cyclic response of the column specimen with good accuracy. The observed

overestimation of strength during the last two cycles can be attributed to bond slip and shear distortion in the plastic hinge region, which cannot be predicted by standard fiber-type element models.

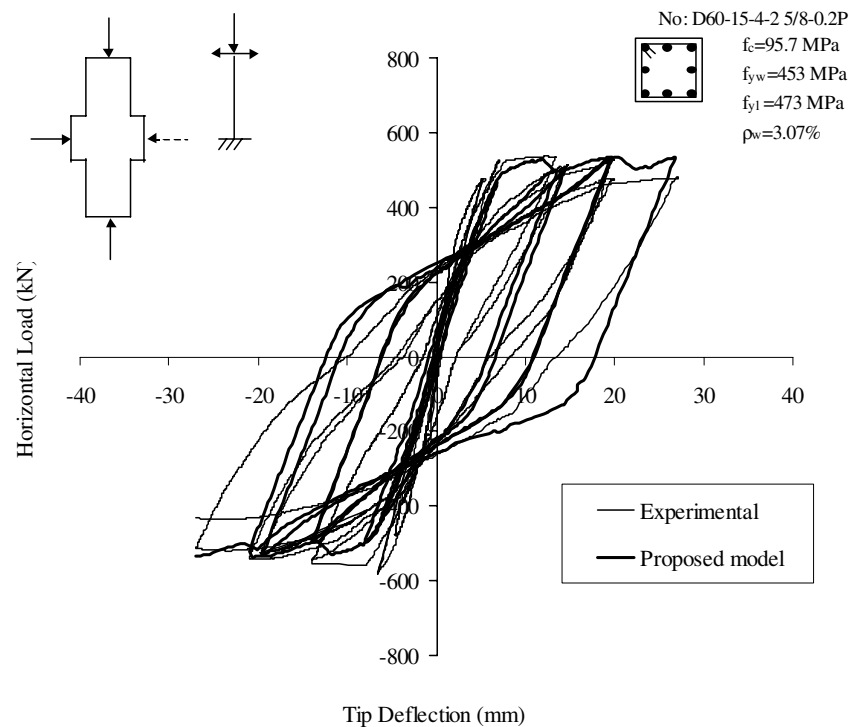


Figure 8. Comparison of analytical predictions and experimental results for specimen D60-15-4-2 5/8-0.2P tested by Azizinamini et al. [18] under cyclic loading

CONCLUSIONS

A model for predicting the response to cyclic loading of HSC members (with and without confinement reinforcement) was developed and implemented within the nonlinear finite element analysis program ADAPTIC. Following verification through a study on the member level, under cyclic loading, it was concluded that the proposed model provides a good fit to a wide range of experimental envelope curves and hysteresis loops, while at the same enabling the assessment of real structural problems in a computationally efficient manner. It appears therefore, that the proposed model can form the basis for analytical modeling of the seismic response of HSC members and structural systems, with behavior dominated by flexure and axial force, under static and dynamic conditions.

ACKNOWLEDGEMENTS

The financial assistance provided by the European Commission within the Environment and Climate Programme (contract no. ENV4-CT96-5027) is gratefully acknowledged.

REFERENCES

1. Penelis GG, Kappos AJ. "Earthquake resistant concrete structures." E & FN SPON (Chapman & Hall), London, 1997.
2. Muguruma H, Watanabe F. "Ductility improvement of high strength concrete columns with lateral reinforcement." Proceedings of the 2nd International Symposium on Utilization of high strength concrete, ACI Special Publication SP 121-4, 47-60, 1990.
3. Karsan ID, Jirsa JO. "Behavior of concrete under compressive loadings." ASCE Journal of Structural Division 1969; 95(12): 2543-2563.
4. Aoyama H, Noguchi H. "Mechanical properties of concrete under load cycles idealizing seismic actions." Bulletin d'Information CEB, 131, 29-63, 1979.
5. Yankelevsky DZ, Reinhardt HW. "Model for cyclic compressive behavior of concrete." Journal of Structural Engineering 1987; 113(2): 228-240.
6. Mander JB, Priestley MJN, Park R. "Theoretical stress-strain model for confined concrete." Journal of Structural Engineering 1988; 114(8): 1804-1826.
7. Otter DE, Naaman AE. "Model for response of concrete to random compressive loads." Journal of Structural Engineering 1989; 115(11): 2794-2809.
8. Martinez-Rueda JE. "Energy dissipation devices for seismic upgrading of RC structures." PhD Thesis, Dept. of Civil Engineering, Imperial College, Univ. of London, London, 1997.
9. Blakeley RWG, Park R. "Prestressed concrete sections with cyclic flexure." ASCE Journal of Structural Division 1973; 99(ST8): 1717-1742.
10. Popovic S. "A numerical approach to the complete stress-strain curve of concrete." Cement and Concrete Research 1973; 3(5): 583-599.
11. Kappos AJ, Konstantinidis D. "Statistical analysis of confined High Strength Concrete." Materials and Structures 1999; 32: 734-748.
12. Bing L, Park R, Tanaka H. "Strength and ductility of reinforced concrete members and frames constructed using high strength concrete." Research Report 94-5, Univ. of Canterbury, New Zealand, 1994.
13. CEB Working Group on HSC/HPC. "High performance concrete, Recommended Extensions to the MC 90 Research Needs." Bulletin d'Information CEB, 228, 1995.
14. Martinez S, Nilson AH, Slate FO. "Spirally reinforced high strength concrete columns." ACI Journal 1984; 81(5): 431-442.
15. Cusson D, Paultre P. "Behavior of high strength concrete columns confined by rectangular ties under concentric loading." Report No. SMS-9202, Dept. of Civil Engineering, Univ. of Sherbrooke, Quebec, Canada, 1993.
16. Sheikh SA, Uzumeri SM. "Analytical model for concrete confinement in tied columns." Journal of Structural Division 1982; 108(ST12): 2703-2722.
17. CEB. "CEB/FIP Model Code 1990." Bulletin d'Information CEB, 213/214, Lausanne, 1993.
18. Azizinamini A, Kuska SSB, Brungardt P, Hatfield E. "Seismic behavior of square high strength concrete columns." ACI Structural Journal 1994; 91(3): 336-345.
19. Izzuddin BA. "Non-linear dynamic analysis of framed structures." PhD thesis, Dept. of Civil Engineering, Imperial College, Univ. of London, London, 1991.
20. Cook JE. "Research and application of high strength concrete: 10000 psi concrete." Concrete International 1989; 11(10): 67-75.